This article has been accepted for inclusion in a future issue of this journal. Content is final as presented, with the exception of pagination.

Walking Speed Learning and Generalization Using Seq2Seq Gated and Adaptive Continuous-Time Recurrent Neural Network (S2S-GACTRNN) for a Hip Exoskeleton

Wuxiang Zhang, *Member, IEEE*, Zhitao Ling, Stefan Heinrich, Xilun Ding, and Yanggang Feng, *Member, IEEE*

***Abstract*—The objective of this article is to provide a new approach for walking speed learning and generalization in the speed-adaptation control of exoskeletons. By combining the gated and adaptive continuous-time recurrent neural network (GACTRNN), which has the potential to process periodic signals, and the "sequence to sequence" structure, the S2S-GACTRNN model is proposed for walking gait generation at different speeds. The "proactive loop" and "reactive loop" were presented for learning and generalization capability evaluation, respectively, in the experiments of sinusoidal signals and walking gait signals. First, simulation experiments were carried out to evaluate the S2S-GACTRNN's learning and generalization capabilities of sinusoidal signals with different frequencies. Second, in offline experiments, the model was applied to deal with walking gait signals to evaluate the capabilities of learning and generalization of walking speeds. Third, a client-server system was constructed and an online prediction method was proposed for online experiments to further evaluate the trained model's performance in walking speed generalization. The mean absolute errors of S2S-GACTRNN trained using walking data at three speeds were reduced by 24%, 38%, and 24% compared with that trained using walking data at one speed. The results show that the model has learning and generalization potential for gait signals of different walking speeds and may be utilized as a new approach to the adaptive control of walking speeds in the field of exoskeletons.**

***Index Terms*—Hip exoskeleton, learning and generalization, recurrent neural network.**

Manuscript received 14 April 2022; revised 5 September 2022; accepted 23 December 2022. Recommended by Technical Editor B. Chu and Senior Editor G. Alici. This work was supported in part by the National Natural Science Foundation of China (NSFC) under Grant 91848104, and in part by the Basic Science Research Grant of Beihang University under Grant KG16115201. *(Corresponding author: Yanggang Feng.)*

This work involved human subjects or animals in its research. Approval of all ethical and experimental procedures and protocols was granted by the Local Ethics Committee of Beihang University, Application No. BM20220209, and performed in line with the Declaration of Helsinki.

Wuxiang Zhang and Xilun Ding are with the School of Mechanical Engineering and Automation, Beihang University, Beijing 100191, China, and also with the Beijing Advanced Innovation Center for Biomedical Engineering, Beihang University, Beijing 100191, China (e-mail: zhangwuxiang@buaa.edu.cn; xlding@buaa.edu.cn).

Zhitao Ling and Yanggang Feng are with the School of Mechanical Engineering and Automation, Beihang University, Beijing 100191, China (e-mail: lingzhitao@buaa.edu.cn; yanggangfeng@buaa.edu.cn).

Stefan Heinrich is with the Department of Computer Science, IT University of Copenhagen, 2300 København, Denmark (e-mail: stehe@itu.dk).

This article has supplementary material provided by the authors and color versions of one or more figures available at https://doi.org/10.1109/TMECH.2022.3233434.

Digital Object Identifier 10.1109/TMECH.2022.3233434

I. Introduction

As a wearable device, lower limb exoskeletons are widely used not only for the rehabilitation treatment of patients with lower limb dysfunction such as paralysis, but also to provide motor assistance for elderly individuals whose physical function declines with age [1], [2], [3], [4]. The performance of the exoskeleton depends on the control system and the matching degree between assistance strategies and users. For users with fully reduced walking ability (e.g., hemiplegia), one control strategy of the exoskeleton is to drive users' legs along a predefined trajectory [5], [6], [7]. However, the exoskeleton faced some challenges while assisting people with walking ability or partial walking ability (e.g., elderly individuals and patients during late recovery after stroke), e.g., reducing muscle activity and causing abnormal muscle activity patterns [8]. In this case, users of the exoskeleton do not always follow a fixed gait trajectory, but adjust their gaits (e.g., walking speed) according to their needs, which requires the exoskeleton to provide partial assistance for lower limb movements. For example, users who normally walk at relatively high speeds may reduce their walking speeds when they become fatigued. In an emergency, the walking movements of users may suddenly stop, causing the exoskeleton to dramatically make adjustments. Consequently, a robust and adaptive method is needed to enable self-dominated gaits for users to move at different walking speeds [9], [10].

One approach to realizing speed adaptation is using model-based methods, i.e., nonneural-networks. A nonlinear decentralized control scheme for a lower-limb exoskeleton was developed to enable the wearers to stabilize the walking speed to the desired value by changing their torso pitch angle [11].

1083-4435 © 2023 IEEE. Personal use is permitted, but republication/redistribution requires IEEE permission.
See https://www.ieee.org/publications/rights/index.html for more information.

Authorized licensed use limited to: BEIHANG UNIVERSITY. Downloaded on February 17,2023 at 11:37:53 UTC from IEEE Xplore. Restrictions apply.

This article has been accepted for inclusion in a future issue of this journal. Content is final as presented, with the exception of pagination.

Although the experimental results show great stabilization and tracking accuracy to the subjects' desired velocities, it remains difficult to real-time control loops due to the high cost of computing resources [12]. Vallery et al. [13] proposed an online-trajectory-generation method, named complementary limb motion estimation (CLME), to generate the reference trajectory of the affected leg via that of the healthy leg by exploiting the physiological inter-joint couplings. The CLME allows subjects to autonomously generate the reference motion, but it may be more suitable for users with at least one leg completely healthy (e.g., hemiplegia). In addition to the information about the healthy parts of individuals, the gaits or muscle states of the assisted leg can be directly processed for the exoskeleton to generate trajectories and to realize speed-adaptation control. The adaptive oscillators (AOs), which are mathematical tools capable of learning features such as the frequency and envelope of a periodic signal, were utilized for trajectory generation [14], [15], [16], [17], [18]. The AOs were put in parallel to construct a pool of AOs for the decomposition and synthesis of walking gaits, to provide a reliable estimation of the trajectory at different speeds [14]. Zheng et al. [15] proposed a gait phase estimation strategy using a noncontact capacitive sensing system and an AOs-based gait phase estimator, to reliably estimate the gait phase from the information of the leg, when the walking speed changes and when the sensing device is reworn. The gait phase estimation performance got improved by utilizing a more simplified sensing system for real-time control of an active exoskeleton [16]. The experiments show that the strategy performed an accurate estimation at different speeds in real time. One premise of the AOs-based trajectory generation method is that the gait trajectory can achieve the desired accuracy through finite synthesis. Due to the inherent fluctuations of walking, the AOs-based method may be sensitive to the tuning of the AOs parameters, especially for a signal with several harmonics [17]. Besides, some measures need to be taken to reduce the adapting time of the AOs. Additionally, dynamic movement primitive (DMP) theory was deployed as a generator for trajectory planning during sit-to-stand motion based on a previously collected database of trajectories as training samples [19]. The parameters in the DMP gait model can be modified to synchronize the DMP trajectory speed with the user's intended speed. One challenge of the DMP gait model is that a complete motion gait cycle or segment is needed to relearn a new DMP model in the process of modeling and learning the users' motion gaits.

The other approach to realizing speed adaptation is using model-free methods, i.e., data-driven neural networks. Essentially, the walking gaits change alongside time changes, which can be regarded as the signals with the features of time series and can be processed by time-series related neural networks [20]. Neural networks have been utilized to extract some useful information from motion patterns in the state of the art [21], [22], [23]. The convolutional neural network was employed to construct a gait phase estimator to modulate exoskeleton assistance through different locomotion mode settings [21]. The graph convolutional network was also applied to recognize the four phases of a one-leg gait during walking for gait phase classification from the nonEuclidean domain [22]. A novel continuous-time recurrent neural network (CTRNN) was proposed and showed the potential to extract stochastic structures hidden in noisy time series data used for training [24]. The variant, named stochastic CTRNN (S-CTRNN), was utilized for a robot to reproduce latent stochastic structures hidden in fluctuating tutoring trajectories [25]. The S-CTRNN was combined with Bayesian inference to analyze drawings of different shapes that can be regarded as multidimensional time series to investigate the underlying cognitive mechanisms between humans and chimpanzees [26].

In our previous study, inspired by the brain's general adaptation and dynamic tuning to sensorimotor information during learning sequential information, we proposed a gated and adaptive CTRNN (GACTRNN) [27], [28]. The timescale value of the GACTRNN steers how strongly or weakly a neuron is leaking, thus how fast or slow it is forgetting its previous activation. The GACTRNN can learn general patterns on multiple timescales that could temporally vary notably because the neurons in the models adapt and modulate their inherent timescale characteristics via current inputs [28], which is similar to the perception and adaption mechanism of brains. Using this mechanism, in this study, we employed the GACTRNN for walking gait prediction at different speeds to show its potential in walking speed generalization. To realize multistep prediction of gaits in the time domain, the "sequence to sequence" (seq2seq) structure (a form of processing while using the recurrent neural network [29]) is combined with the GACTRNN, to construct the seq2seq GACTRNN (S2S-GACTRNN) for time-series processing.

The contributions of this study are to propose the S2S-GACTRNN which is based on the "sequence to sequence" structure and the GACTRNN, whose perception and adaptation mechanism is similar to that of the brain, and to apply the proposed network for walking speed learning and generalization in the field of exoskeletons using the "proactive loop" and "reactive loop". Simulation experiments of sinusoidal signals with different frequencies, and offline experiments and online experiments of walking gait signals at different speeds were carried out to evaluate the model's learning and generalization capability. The overview of this study is shown in Fig. 1.

II. S2S-GACTRNN and Experimental Platform

In terms of gait prediction, the GACTRNN model is needed to process the gaits from the previous period and to predict the gaits in the subsequent period. To achieve a more reasonable sequence prediction, the input and prediction sequence of the model should retain their time sequence information, and both the input process and generation process must be in order. Therefore, the seq2seq structure is combined with GACTRNN to build the network model in this article. Moreover, the experimental platform is described in this section.

A. S2S-GACTRNN

1) Model: The hybrid S2S-GACTRNN, unfolded by time steps, is shown in Fig. 2. The seq2seq model, including an encoder and a decoder, is a form of processing while using the RNN, whose input sequence and output sequence may not have

Authorized licensed use limited to: BEIHANG UNIVERSITY. Downloaded on February 17,2023 at 11:37:53 UTC from IEEE Xplore. Restrictions apply.

This article has been accepted for inclusion in a future issue of this journal. Content is final as presented, with the exception of pagination.

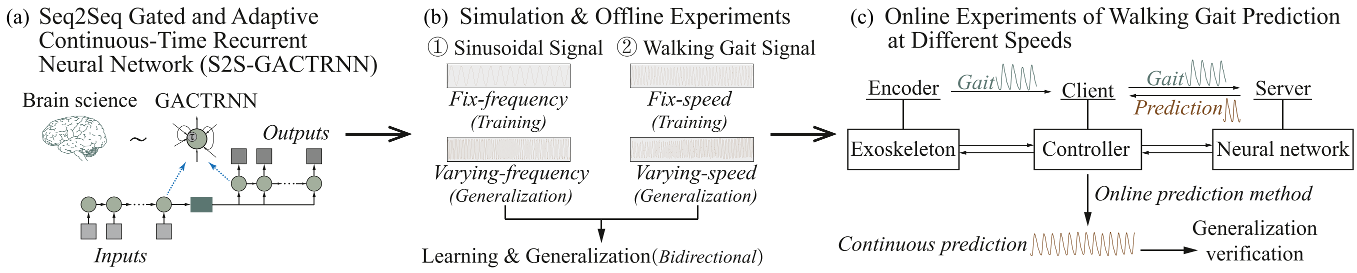
(a) Seq2Seq Gated and Adaptive Continuous-Time Recurrent Neural Network (S2S-GACTRNN)
Brain science
GACTRNN
~
Outputs
Inputs
(b) Simulation & Offline Experiments
① Sinusoidal Signal
② Walking Gait Signal
Fix-frequency (Training)
Fix-speed (Training)
Varying-frequency (Generalization)
Varying-speed (Generalization)
Learning & Generalization (Bidirectional)
(c) Online Experiments of Walking Gait Prediction at Different Speeds
Encoder
Gait
Client
Gait
Prediction
Server
Exoskeleton
Controller
Neural network
Online prediction method
Continuous prediction
Generalization verification

Fig. 1. Overview of this study. (a) S2S-GACTRNN model inspired by brain science. (b) Simulation and offline experiments using sinusoidal signals and walking data from three subjects to evaluate S2S-GACTRNN's learning and generalization capabilities. (c) Online walking experiments at different speeds to further verify the trained model's generalization capability.

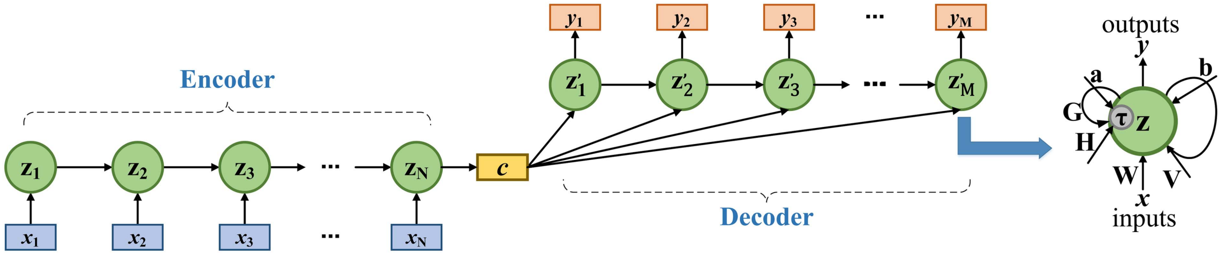

Fig. 2. S2S-GACTRNN model includes an encoder and a decoder. $\{\boldsymbol{x}_i\}$ and $\{\boldsymbol{y}_i\}$ are the input and output sequences, respectively. $\mathbf{z}_t$ and $\mathbf{z}'_t$ are the internal states of the encoder and decoder, respectively. $\boldsymbol{c}$ represents the context vector that contains the information of the input sequence. Each unit (green circles) is a GACTRNN unit whose computational mechanism is shown on the right.

the same length [30]. The input sequence $\{\boldsymbol{x}_i\}$ is chronologically fed and encoded into the context vector $\boldsymbol{c}$, which contains the input information. The vector $\boldsymbol{c}$ is used as input of the decoder at each time step in the decoding process to generate the output sequence $\{\boldsymbol{y}_i\}$ afterward. N and M represent the length of the input sequence and the length of the output sequence, respectively. Since vector $\boldsymbol{c}$ contains the hidden feature information of the input sequence and is used in each time step of the decoding process, the generated sequence can be considered a comprehensive prediction of the input sequence.

Each unit in the S2S-GACTRNN model is a GACTRNN unit, whose characteristic is shown on the right side of Fig. 2. In tasks with discrete numbers of time steps, the GACTRNN can be employed as a discrete model. As a result, the activation $\mathbf{y}$ of GACTRNN units is defined as follows:

$$\mathbf{y}_t = f\left(\mathbf{z}_t\right) \tag{1}$$

$$\mathbf{z}_t = \left(1 - \frac{1}{\boldsymbol{\tau}_t}\right)\mathbf{z}_{t-1} + \frac{1}{\boldsymbol{\tau}_t}\left(\mathbf{W}\mathbf{x} + \mathbf{V}\mathbf{y}_{t-1} + \mathbf{b}\right) \tag{2}$$

$$\boldsymbol{\tau}_t = 1 + \exp\left(\mathbf{H}\mathbf{x} + \mathbf{G}\mathbf{y}_{t-1} + \mathbf{a} + \boldsymbol{\tau}_0\right) \tag{3}$$

for inputs $\mathbf{x}$, internal states $\mathbf{z}_t$ at time step t and previous internal states $\mathbf{z}_{t-1}$, weights $\mathbf{W}$ and $\mathbf{V}$, and bias $\mathbf{b}$. f represents the activation function: $\tanh(x) = \frac{e^x - e^{-x}}{e^x + e^{-x}}$. The *timescale* parameter $\boldsymbol{\tau}_t$ expresses the leakage of neurons, which can be a scalar or vector. The constant $\boldsymbol{\tau}_0$ can be computed by the initial value of the *timescale* parameter $\boldsymbol{\tau}$ before training: $\boldsymbol{\tau}_0 = log(\boldsymbol{\tau} - 1)$. Compared with the CTRNN, the additional trainable parameters are introduced in the GACTRNN to complete the gated and adaptive characteristics: $\mathbf{H}$, $\mathbf{G}$, and $\mathbf{a}$, which represent the input weights, recurrent weights, and bias on the timescale, respectively. The external input $\mathbf{x}$ was fed to the model at each time step and multiplied by $\mathbf{H}$, to modulate the timescale $\boldsymbol{\tau}_t$. Since $\mathbf{H}$ is directly related to the input $\mathbf{x}$, the GACTRNN may adjust the leakage of the internal state according to the current external input x and may have a stronger capability for processing cyclic signals compared with the CTRNN.

The GACTRNN neurons can be grouped into several *modules* and share the same timescale in each module [28]. All these modules are recurrently interconnected using a *dense* strategy. For example, an encoder with (m_1, m_2, m_3, m_4) neurons with timescales (τ_1, τ_2, τ_3, τ_4) means that the encoder has four modules of different sizes with their initial values of timescales. In this study, to simplify the model, both the encoder and decoder share the same number of modules and neurons, as well as the timescales. "MSE" and "RMSProp" are selected as the loss function and optimizer, respectively, for model training.

2) Proactive Loop & Reactive Loop: After being trained by datasets, the network can generate the output sequence as predictions of the previous input sequence. To evaluate the model's characteristics, there are two different ways (refer to Fig. 3) to generate predictions depending on the kth input sequence $\left\{\boldsymbol{x}_i^{(k)}\right\}$

a) Proactive loop

$$\boldsymbol{x}_i^{(k)} = \begin{cases} \boldsymbol{x}_{i+\mathrm{M}}^{(k-1)}, 1 \le i \le \mathrm{N} - \mathrm{M} \\ \boldsymbol{y}_{i+\mathrm{M}-\mathrm{N}}^{(k-1)}, \mathrm{N} - \mathrm{M} + 1 \le i \le \mathrm{N} \end{cases} \tag{4}$$

This article has been accepted for inclusion in a future issue of this journal. Content is final as presented, with the exception of pagination.

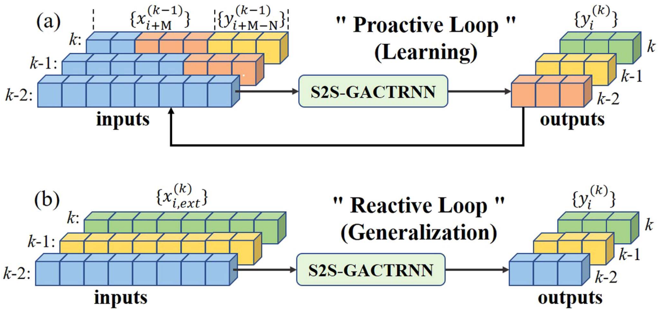

Fig. 3. Two generation methods. (a) Proactive loop related to learning capability. The kth input sequence $\{\boldsymbol{x}_i^{(k)}\}$ consists of two parts: The latter part of the inputs $\{\boldsymbol{x}_i^{(k-1)}\}$ (blue and orange cubes) and the whole outputs $\{\boldsymbol{y}_i^{(k-1)}\}$ of the $(k-1)$th prediction (yellow cubes). (b) Reactive loop related to generalization capability. The current inputs are the external inputs.

where N and M represent the length of the input sequence and the length of the output sequence, respectively. $\boldsymbol{x}_{i+\mathrm{M}}^{(k-1)}$, $\boldsymbol{y}_{i+\mathrm{M}-\mathrm{N}}^{(k-1)}$ represents the input at time step $i+\mathrm{M}$ and the output at time step $i+\mathrm{M}-\mathrm{N}$, respectively, of the $(k-1)$th prediction.

b) Reactive loop

$$\boldsymbol{x}_i^{(k)} = \boldsymbol{x}_{i,ext}^{(k)}, 1 \leq i \leq \mathrm{N} \tag{5}$$

where $\boldsymbol{x}_{i,ext}^{(k)}$ represents the external input at time step i of the kth prediction.

In the "proactive loop", the kth input sequence $\{\boldsymbol{x}_i^{(k)}\}$ consists of two parts: The latter part of the inputs $\{\boldsymbol{x}_i^{(k-1)}\}$ and the whole outputs $\{\boldsymbol{y}_i^{(k-1)}\}$ of the $(k-1)$th prediction. The $(k-1)$th outputs of the network are used for the kth prediction (like a closed loop), which means that no external inputs will be needed in subsequent predictions except for the first prediction. This method is deployed to evaluate the learning capability in the following experiments.

The "reactive loop" is commonly employed in neural networks. The current external signals are fed to the network as inputs to make a prediction. This method is deployed to evaluate the generalization capability in the following experiments.

B. Experimental Platform

A hip joint exoskeleton is utilized in the experiments. The exoskeleton comprised a 3-DOF concentric series mechanism, novel series elastic actuator (SEA), thigh bar, and 3-D printed component, with an active flexion-extension degree of freedom on the sagittal plane and two passive degrees of freedom on the axial and coronal planes (refer to Fig. 4). The thigh bar is driven by the SEA and can be bundled to the wearer's thigh with the 3-D printed component and bandages. The SEA includes a frameless motor, harmonic reducer, and constant-stiffness torsion spring, on either side of which a rotary magnetic encoder is installed for angle measurement (motor encoder and joint encoder). The hip joint angle can be obtained by the encoder and the output torque of the SEA can be calculated by Hooke's law. An experimental platform is built for the subsequent exoskeleton experiments, as shown in Fig. 5. The hip joint exoskeleton is fixed to a supporting frame with a treadmill below it. The supporting frame is equipped with a ball screw mechanism, which allows subjects to adjust the exoskeleton to the heights corresponding to their leg lengths. The control system hardware is integrated into a box and installed behind the exoskeleton. The speed of the treadmill can be regulated from 0.1 to 10.0 km/h with a minimum speed interval of 0.1 km/h. The treadmill control panel is equipped with a clock for timing the experiments.

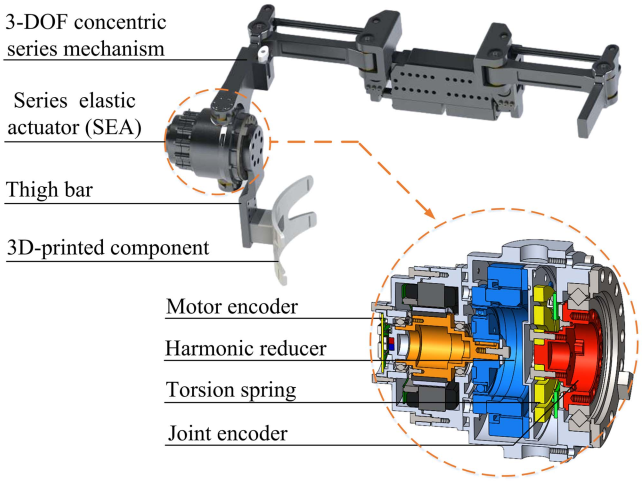

Fig. 4. Hip joint exoskeleton and series elastic actuator (SEA).

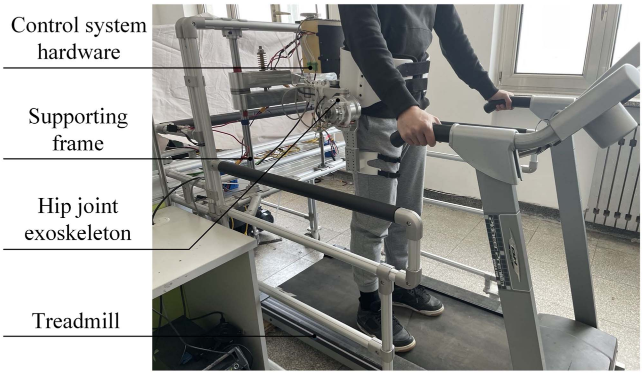

Fig. 5. Experimental platform includes a hip exoskeleton, a frame for supporting, a box with integrated control system hardware, and a treadmill.

III. Simulation and Offline Experiments

The GACTRNN model is inspired by brain science and has been verified to capture patterns and underlying temporal characteristics from input sequences. For example, the model can generate different whole Lissajous shapes according to only their initial curves [28]. Therefore, a trained model can learn some characteristics of the training data and contain prior experience with the training data. Similarly, as a variant, it is necessary to evaluate this "learning capability" of the S2S-GACTRNN model. The "proactive loop" mode of the model will be employed to generate continuous sequence prediction

Authorized licensed use limited to: BEIHANG UNIVERSITY. Downloaded on February 17,2023 at 11:37:53 UTC from IEEE Xplore. Restrictions apply.

This article has been accepted for inclusion in a future issue of this journal. Content is final as presented, with the exception of pagination.

and the learning capability of the model will be verified by the reproduction of the characteristics of the training signals.

Additionally, the generalization capability of the neural network is worthy of attention when building and training a network, which essentially refers to the ability of the model to learn from given data and apply what the model has learned elsewhere. Generalization is one of the features most useful and specific to neural networks [31]. Similarly, for the S2S-GACTRNN model built in this article, we use the trained model to make predictions for the external inputs with different signal characteristics (in "reactive loop" mode) and investigate the prediction and generalization errors of S2S-GACTRNN to verify the generalization capability.

Generally, the performance of neural networks is related to the scale and the amount of training data. In this study, using the data from simulation and real-world walking for training, the S2S-GACTRNN model's learning and generalization capabilities of periodic signals on small-scale datasets were investigated. First, simulation experiments with sinusoidal signals were carried out to verify S2S-GACTRNN's ability to process periodic signals with different frequencies. Subsequently, the model was used to process a more complex period signal—the walking gait signal, which may have varying frequency and amplitude with walking speed. The offline experiments using real-world walking data were carried out to evaluate the model's learning and generalization capabilities of walking gait signals at different speeds, to show S2S-GACTRNN's potential for adaptive speed control.

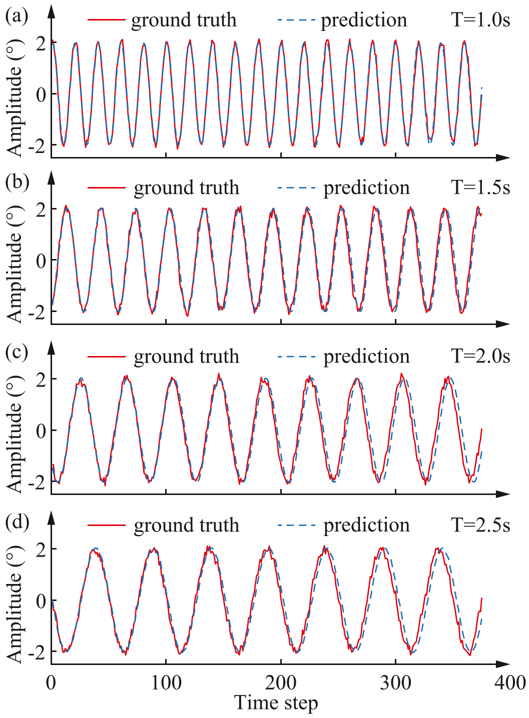

Fig. 6. Predictions of sinusoidal signals with different periods in the "proactive loop" $y = 2\sin\left(\frac{2\pi}{\mathrm{T}}t\right) + \mathrm{N}\left(0, 0.1^2\right)$. (a) T = 1.0 s. (b) T = 1.5 s. (c) T = 2.0 s. (d) T = 2.5 s.

A. Simulation Experiments of Sinusoidal Signals

1) Data Acquisition: The sinusoidal signals include the fixed-frequency signal (FFS) for network training and learning evaluation and the varying-frequency signal (VFS) for generalization evaluation. Both kinds of signals are generated by

$$y = 2\sin\left(\frac{2\pi}{\mathrm{T}}t\right) + \mathrm{N}\left(0, 0.1^2\right) \tag{6}$$

where T is the signal period, $\mathrm{N}\left(0, 0.1^2\right)$ is Gaussian noise with a mean value of 0 and standard deviation of 0.1, and t is the time length. The signal sampling time is set to 50 milliseconds. For FFS and VFS, parameter T is set to

a) *FFS (for training and learning evaluation):* $\mathrm{T} = \mathrm{T}_1, \mathrm{T}_2, \mathrm{T}_3, \ldots$. A dataset of training data is generated for each T_i. In this way, several datasets of different fixed periods are obtained for model training and learning capability evaluation in the "proactive loop".

b) *VFS (for generalization evaluation):* T = 1.2 s, 1.3 s, . . ., 2.4 s. By generating a five-cycle signal for each T (setting t = 5 T) and splicing them in order of ascending period, a dataset of sinusoidal signals with different frequencies is obtained for model generalization in the "reactive loop".

2) Learning Capability: We used four datasets of FFS with T = 1.0 s, 1.5 s, 2.0 s, and 2.5 s (all the time lengths were set to t = 60 s) to train a model with (6, 6, 6, 6) neurons and timescales (1, 3, 9, 27). The length of the input sequence and the length of the output sequence were set to N=25 and M=3, respectively. Subsequently, the initial values of another four sinusoidal signals with the above signal periods were fed to the trained model and the predictions were generated in the "proactive loop". The results showed that the trained model was able to reproduce the whole sinusoidal signals with different periods via the initial values of signals (refer to Fig. 6), which meant that the model gained some prior knowledge from the training sets and that the S2S-GACTRNN model had a certain capability of learning the characteristics of sinusoidal signals with different periods. In addition, due to the prediction errors, the accumulation of errors would cause the generated curve to deviate from the actual curve more significantly deviating with future time steps.

3) Generalization Capability: To evaluate the generalization capability, two S2S-GACTRNN models were obtained by using different training data–the first model was trained by one dataset of FFS with T = 1.8 s (set to t = 60 s), while the second model was trained by three datasets of FFS with T = 1.7 s, 1.8 s, and 1.9 s (also set to t = 60 s). The length of the input sequence and the length of the output sequence were set to N = 25 and M = 3, respectively. Both models shared the same hyperparameters: (6, 6, 6, 6) neurons with timescales (1, 5, 25, 125), and 15% of the training data were split for model validation during training.

Since the VFS contains sinusoidal signals with a wider range of periods (T = 1.2 s, 1.3 s,..., 2.4 s) than FFS, applying trained models (the first model was trained by FFS with T = 1.8 s, and the second model was trained by FFS with T = 1.7 s, 1.8 s, and 1.9 s) for the prediction of VFS can help evaluate the model's

Authorized licensed use limited to: BEIHANG UNIVERSITY. Downloaded on February 17,2023 at 11:37:53 UTC from IEEE Xplore. Restrictions apply.

This article has been accepted for inclusion in a future issue of this journal. Content is final as presented, with the exception of pagination.

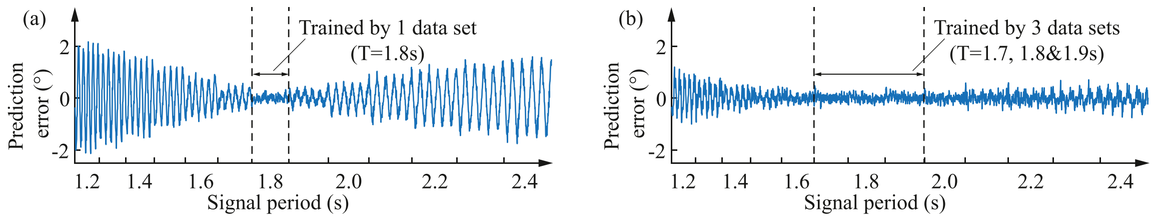

Fig. 7. Prediction error of the simulation experiments of varying-frequency signals. (a) Model is trained by 1 dataset. (b) Model is trained by 3 datasets.

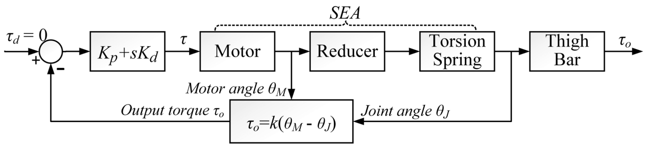

Fig. 8. Block diagram of the transparent mode based on the PD controller.

generalization capability with the guideline that a lower prediction error means a stronger generalization capability. The errors between the prediction and the ground truth were calculated to evaluate the prediction accuracy, as shown in Fig. 7. Both models performed better in predicting the sinusoidal signals at the periods of their training signals (T = 1.8 s and T = 1.7 s, 1.8 s, and 1.9 s, respectively) compared with other periods. With an increase in signal period deviation, the prediction errors of the two models also gradually increased (both increasing direction and decreasing direction), meaning that the generalization capability of the model declined. Moreover, by comparing the two error curves, the generalization errors of the model trained by three datasets of FFS were significantly smaller than those trained by only one dataset of FFS. The results indicate that the S2S-GACTRNN model has potential capability in the prediction task of sinusoidal signals with different frequencies and that the generalization capability can be improved by using more datasets in model training.

B. Offline Experiments of Walking Gait Signals

1) Data Acquisition: To obtain the data on human walking gaits, we carried out experiments in which the subjects walked on a treadmill wearing the exoskeleton. The exoskeleton worked in the transparent mode based on the PD controller with the joint torque τ_o calculated for feedback (refer to Fig. 8), which had minimum output impedance, allowing the user to freely move while walking [32]. Gravity compensation was not employed for the control due to the small quality of the thigh bar. The other two passive degrees of freedom of the hip joint exoskeleton were restricted in case of disturbance. The data from the encoder were collected with a sampling rate of 100 Hz and the hip joint angle values were calculated and recorded. Two types of gait signals are collected

a) *Fixed-speed signal (FSS, for training and learning evaluation):* The subject walked on the treadmill for 60 s at a fixed speed during one data acquisition experiment. Several datasets of walking gaits at different fixed walking speeds were obtained for model training and learning capability evaluation in the "proactive loop".

b) *Varying-speed signal (VSS, for generalization evaluation):* The subject walked at an initial speed of v = 1.0 km/h, and subsequently, the speed was manually increased by 0.2 km/h until 3.0 km/h every 10 s via a control panel. One dataset of walking gaits at varying walking speeds was obtained for model generalization in the "reactive loop".

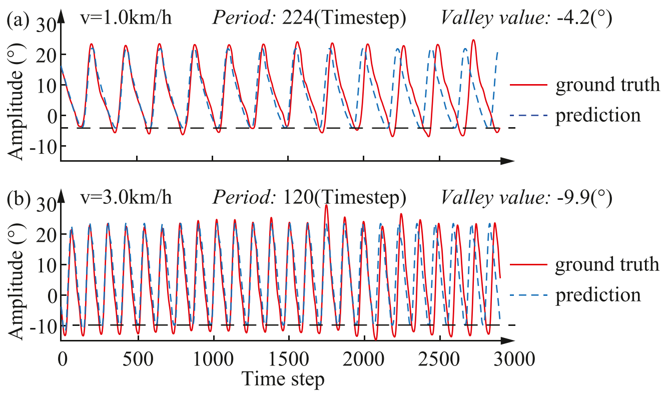

Fig. 9. Predictions of walking gait signals at v = 1.0 km/h and 3.0 km/h in the "proactive loop". The trained model reproduced the corresponding frequencies (or periods) and valley values of walking gaits.

2) Learning Capability: Two datasets of FSS with v=1.0 km/h and 3.0 km/h were utilized in this experiment, and both time lengths were set to t = 600 s. The step size of the sliding window for dataset construction was set to 10 to simplify training. These two datasets were selected to train a network with (16, 16, 16, 16) neurons and timescales (1, 6, 36, 216). The length of the input sequence and the length of the output sequence were set to N = 100 and M = 10, respectively. After training, the initial values of another two walking gait signals at the above walking speeds were input to the model to generate a prediction in the "proactive loop". As shown in Fig. 9, both prediction curves reproduced the characteristics of their gait signals to a certain extent, including amplitude and frequency. Similar to the sinusoidal simulation experiments, the prediction value increasingly deviated from the ground truth, which may be attributed to the accumulation of errors and the instability of gaits in the process of walking. The experimental results showed that the trained model can learn

Authorized licensed use limited to: BEIHANG UNIVERSITY. Downloaded on February 17,2023 at 11:37:53 UTC from IEEE Xplore. Restrictions apply.

This article has been accepted for inclusion in a future issue of this journal. Content is final as presented, with the exception of pagination.

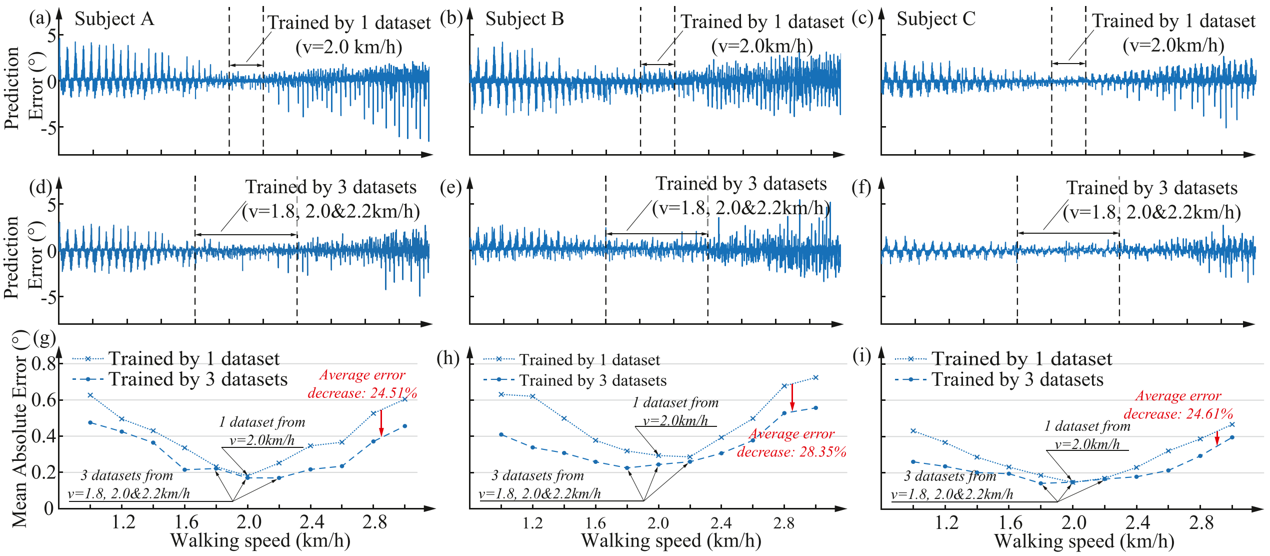

Fig. 10. Prediction results of the offline experiments of the varying-speed signal. (a)(b)(c): Model is trained by 1 dataset. (d)(e)(f): Model is trained by 3 datasets. (g)(h)(i): Mean absolute errors of predictions. (a)(d)(g), (b)(e)(h), (c)(f)(i) are the online results of subject A, B, C, respectively.

TABLE I
PARTICIPANT INFORMATION

Subject	A	B	C
Age (years)	23	24	23
Height (cm)	175	180	177
Weight (kg)	68	70	65
Length of leg (cm)	91	103	99

and reproduce different gaits at two speeds (v = 1.0, 3.0 km/h), respectively.

Overall, we make two noteworthy observations. First, the model effectively learned the frequencies of the two walking gait signals. Second, the model reproduced the corresponding valley values to a certain extent for the two signals, which indicates that the model also has a certain capability of learning the amplitude of walking gait signals.

3) Generalization Capability: Similar to the sinusoidal signal experiments, two S2S-GACTRNN models were trained by different data for generalization capability evaluation—the first model by FSS at a speed of v = 2.0 km/h and the second model by FSS of v = 1.8, 2.0, and 2.2 km/h (3 datasets in total). Considering that the sampling time of the walking gait signals was 10 milliseconds, we set the length of the input sequence and the length of the output sequence to N=100 and M=10, respectively, meaning that the trained models were intended to predict the walking gaits of the next 0.1 s via the gaits of the previous 1 s. The hyperparameters were set to (20, 16, 12, 8) neurons with timescales (1, 6, 36, 216).

After training, both models were then applied for the prediction of VSS. We conducted the same experiments with different subjects (represented by A, B, and C; refer to Table I). The experiments were approved by the Local Ethics Committee of Beihang University. All the subjects read and signed informed consent forms before the experiments.

The prediction results are shown in Fig. 10. Both models performed better in predicting the walking gait signals at the speeds of their training signals (v = 2.0 km/h and v = 1.8, 2.0, and 2.2 km/h) compared with other speeds. Moreover, although VSS is more complex than VFS due to the varying frequency and amplitude with varying walking speeds, by comparing these two models' performance on VSS, we can understand the S2S-GACTRNN model's capability and the implications of the number of training datasets. The mean absolute error (MAE) of prediction at each speed was calculated for analysis [refer to Fig. 10(g)–(i)]. Both models' errors increased with an increase in the speed deviation (both increasing direction and decreasing direction). Additionally, the average generalization errors of the model trained by three datasets of FSS were reduced by 24.51%, 28.35%, and 24.61% compared with those trained by only one dataset of FSS, indicating that the generalization capability of the S2S-GACTRNN model can be improved by more training data.

IV. Online Walking Gait Prediction Experiments

In the above offline experiments, the walking gait signals of each subject were employed for model training. The S2S-GACTRNN model's generalization capability of processing walking gait signals at different speeds was verified. In this section, online prediction experiments were conducted using the previously trained models (2 models for each subject) to further verify the trained model's generalization capability.

A. System Architecture & Online Prediction Method

Since the neural network and motion controller ran on different devices, a client-server system was constructed for the transmission of the real-time and prediction gait data (refer to Fig. 11). A server was deployed on an upper computer (PC), on which the neural network ran in an infinite loop awaiting requests

Authorized licensed use limited to: BEIHANG UNIVERSITY. Downloaded on February 17,2023 at 11:37:53 UTC from IEEE Xplore. Restrictions apply.

This article has been accepted for inclusion in a future issue of this journal. Content is final as presented, with the exception of pagination.

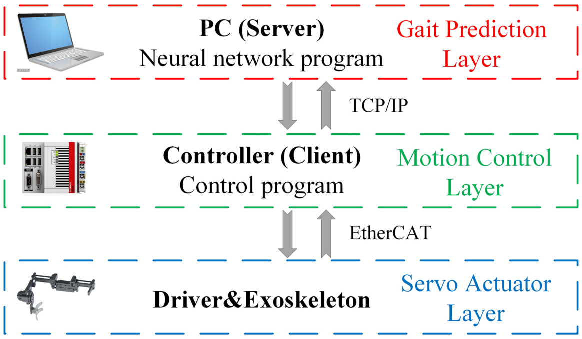

Fig. 11. System architecture: A client-server system was constructed to realize the transmission of the real-time and prediction gait data.

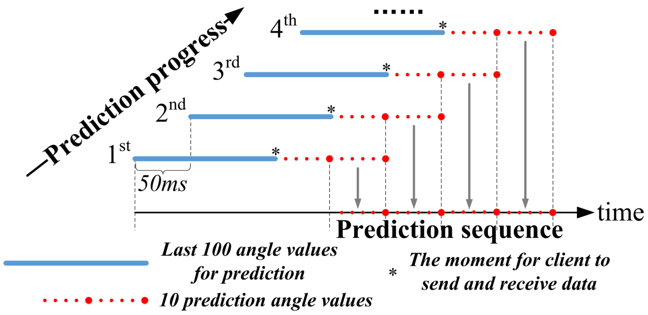
Prediction progress
1st
2nd
3rd
4th
......
50ms
time
Prediction sequence
Last 100 angle values for prediction
10 prediction angle values
The moment for client to send and receive data

Fig. 12. Online prediction method: All the prediction sequences (red dots) were segmented and spliced to generate a continuous sequence.

from the client. The lower computer, which works for the motion control to keep the exoskeleton in the abovementioned transparent mode, deployed a client in charge of acquiring gait signals from the joint encoder and transmitting them to the server. The transmission between the server and the client was based on the TCP/IP protocols. A complete prediction process is described as follows:

1) *Signal acquisition:* When the subject was walking on the treadmill wearing the exoskeleton, the motion controller always computed and recorded the last 100 hip-joint-angle values from the joint encoder (via the EtherCAT protocol) at a sampling time of 10 milliseconds as gait signals for transmission.
2) *Data transmission:* While making a prediction (the timing is described below), the motion controller packs and transmits the 100-angle-value data from the client to the server via the TCP/IP protocol.
3) *Gait prediction:* Once the server receives data, an unpacking and predicting process is conducted by the neural network, and 10 prediction gait angle values are generated. These 10 values are packed and transmitted back to the client. Next, the motion controller obtained the prediction gaits by unpacking the received data.

Considering that both data transmission and forward propagation of the neural network prediction were time consuming, the sequence obtained from each prediction was segmented and spliced to generate a continuous sequence, as depicted in Fig. 12. Since the sampling time was 10 milliseconds, the client was set to transmit data (blue lines) to the server every 50 milliseconds and simultaneously received the last prediction values (10 red dots after each blue line) from the server. The moment is marked with asterisks. The last 5 prediction values generated in each prediction process were used to form a time-continuous sequence.

B. Experimental Process

The same three subjects were recruited to participate in the online walking gait prediction experiments to further verify the generalization capability of the trained models. Similar to the offline experiments, in each subject's online experiments, two neural network models were utilized for data prediction trained by their respective walking data–the first model by FSS at a speed of v = 2.0 km/h and the second model by FSS of v = 1.8, 2.0, and 2.2 km/h. First, the server and client started and the exoskeleton was set to the PD controller-based transparent mode. Subsequently, the subject walked on the treadmill wearing the exoskeleton at an initial speed of v=1.0 km/h. When the walking became smooth, we sent a request from the client to the server for connection establishment. After a short wait for the connection to stabilize, the client started to send real-time gait data and receive prediction values every 50 ms. We used the treadmill clock to time the walking and increased the speed of the treadmill by 0.2 km/h every 10 s by pressing the acceleration button on the control panel. After the subject walked at a speed of 3.0 km/h for 10 s, the client was manually terminated and one experiment was finished. During the experiment, the motion controller generated a continuous sequence of predictions via the above method and saved all the necessary data via the data storage channel. After each experiment, a transmitted and received data comparison was carried out to check whether data packet loss occurred and to ensure the effectiveness of the data.

C. Results

The generalization capability of S2S-GACTRNN was evaluated by the errors (refer to Fig. 13) between the prediction value and the ground truth. We calculated the mean absolute error at each speed, as shown in Fig. 13(g)–(i). The error curves of the online experiments are similar to those of the offline experiments. When walking at speeds corresponding to those of the gaits used in model training (v=2.0 km/h and v=1.8, 2.0, and 2.2 km/h, respectively), the prediction errors were lower than the prediction errors that occurred at other speeds. As the walking speed gradually deviated from the training speed, the prediction error gradually increased. Moreover, from a comparison of the results, the overall generalization errors of the model trained by three datasets of gait signals with different speeds were reduced by 24.08%, 37.99%, and 24.04% compared with that trained by one dataset of gait signals, indicating that the generalization capability of the S2S-GACTRNN was improved with the increase in training data. Overall, the trained model's generalization capability of gait signals was verified by online experiments, indicating that the S2S-GACTRNN model has the potential to process walking gaits at different speeds.

Authorized licensed use limited to: BEIHANG UNIVERSITY. Downloaded on February 17,2023 at 11:37:53 UTC from IEEE Xplore. Restrictions apply.

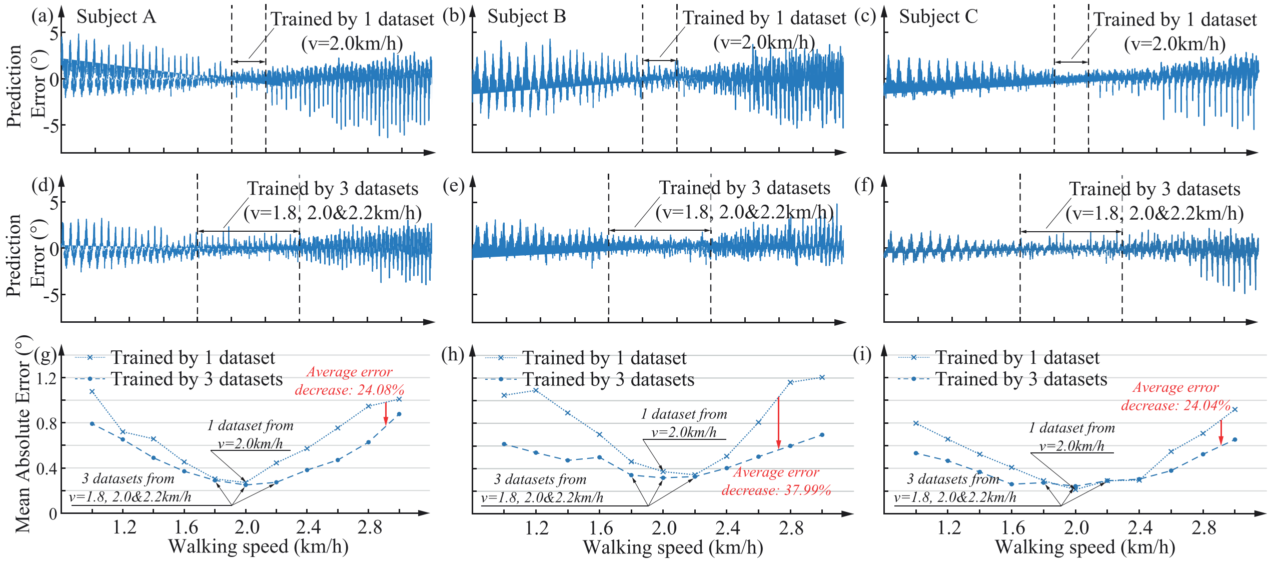

Fig. 13. Prediction results of the online experiments of the varying-speed signal. (a)(b)(c): Model is trained by 1 dataset. (d)(e)(f): Model is trained by 3 datasets. (g)(h)(i): Mean absolute errors of predictions. (a)(d)(g), (b)(e)(h), (c)(f)(i) are the online results of subject A, B, C, respectively.

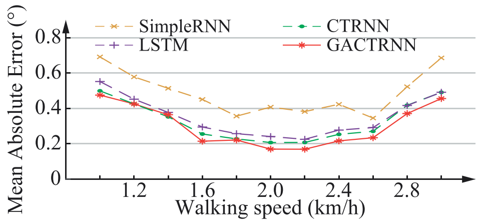

Fig. 14. Performance of SimpleRNN, LSTM, CTRNN, and GACTRNN.

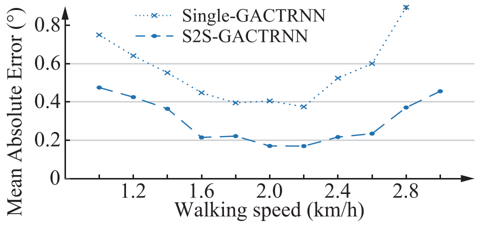

Fig. 15. Performance of Single-GACTRNN (without seq2seq) and S2S-GACTRNN (with the seq2seq structure).

V. Discussion

A. Methods Comparison

The DMP theory is one method for trajectory generation [19]. While using DMP, a complete cycle or segment of the signals is needed for parameter learning. However, the proposed S2S-GACTRNN can make predictions for walking gaits of the next 0.1 s via the gaits of the previous 1 s, which allows it to be more flexibly employed. Another way to generate trajectories is the adaptive oscillator [14], which is similar to a real-time Fourier decomposition. However, a trained S2S-GACTRNN makes predictions based on prior experience and external inputs similar to the brain, while the adaptive oscillator is based on only external inputs. Therefore, compared with the adaptive oscillator, S2S-GACTRNN may have some characteristics of the brain and may be biologically reasonable.

Comparative experiments were also conducted to present the generalization capability of the S2S-GACTRNN with regard to other networks. Three other neurons (simple recurrent neural network (SimpleRNN), Long Short-Term Memory (LSTM), and CTRNN) were used to construct networks using the “seq2seq” structure with the same number of neurons. After trained by FSS of v=1.8, 2.0, and 2.2 km/h, the networks were applied for the prediction of VSS (refer to Fig. 14). The MAEs of the SimpleRNN, LSTM, CTRNN, and GACTRNN are 0.54°, 0.39°, 0.36°, and 0.33° for all speeds, indicating that the GACTRNN neuron may have a greater capability of walking speed generalization.

The S2S-GACTRNN model proposed in this article is a combination of the “seq2seq” structure and GACTRNN. An ablation experiment was conducted to analyze the effect of using the “seq2seq” structure on model performance (refer to Fig. 15). The MAE of the Single-GACTRNN (without seq2seq) is higher than the MAE of the S2S-GACTRNN (with the seq2seq structure) at each walking speed, indicating that the seq2seq structure can help improve network performance.

B. Similarities Between the Brain and the S2S-GACTRNN

The development of brain science is important to the analysis of biological behaviors [33]. In the process of perception of the outside world, biological individuals constantly collect and learn from information to form their cognition of the environment, which will be stored in the brain as prior knowledge to guide their movements [34]. The brain seems to perform this task by learning from perception and actions on different timescales and by well adapting to changing temporal variance [35]. In particular, the brain exhibits temporal abstraction

This article has been accepted for inclusion in a future issue of this journal. Content is final as presented, with the exception of pagination.

and compositionality characteristics that seem to emerge from intrinsic timescale properties in neuromodulation, as well as mode coupling between two neurons across the cortex [36], [37]. This combination of prior experience and sensory inputs has been applied to explain key features of autism [38]. To some extent, the application of the proposed S2S-GACTRNN model to walking gait processing draws lessons from brain science research. Similar to the brain, S2S-GACTRNN learns certain characteristics of signals and obtains prior experience through model training. Specifically, the network learns to represent components of those signals and simultaneously learns to flexibly vary the temporal extent of such components by modulating the timescales. In this way, the model can recognize differences in the timescales of the perceived signal and dynamically adapt its activation. When applied to a prediction task, a trained model makes inferences about the external input signals using the learned knowledge. This mechanism of prior experience and external inputs provides S2S-GACTRNN with the generalization capability of processing biological signals, e.g., walking speed generalization.

C. Characteristics of S2S-GACTRNN

The experimental results show that the proposed model has the potential for generalization while processing human walking gaits at different speeds, which may be improved by using more training data. Considering that only walking gaits are needed, this generalization method only needs to use an encoder for angle measurement without using other sensors (EMG, EEG, IMU, etc.) [39], which may introduce convenience to the application of exoskeletons and avoid difficulties in multisensor fusion algorithm design [40]. Since the results showed the potential of the S2S-GACTRNN in walking speed generalization, the proposed model may be used as a new approach to the adaptive control of the wearer's different walking speeds in the field of exoskeletons. For example, the model can be employed to design a speed adaptive controller to provide suitable assistance for elderly individuals or patients with lower limb motor dysfunction to walk at different speeds. Second, in addition to evaluating the generalization capability of flat-ground walking gaits at different speeds, by optimizing the structure and parameters, the application scenarios of the model may be extended. For example, the proposed model may be used to process the walking gaits of different terrains.

D. Robustness

Some external disturbances (including force and measurement error) may be encountered during experiments, which may affect the results. Since the exoskeleton works in transparent mode, the force disturbance can be considered to have a slight influence on the experiments. However, even with accurate sensors and appropriate filtering algorithms, angle measurement error is difficult to avoid. Therefore, a robustness test was carried out. Gaussian noise $\mathrm{N}\left(\mu, \sigma^2\right)$ was added to the input data of the trained network every 100 ms to simulate the angle measurement error of the discontinuity type. As shown in Fig. 16, the MAE slightly increases when σ is lower than 1.00, which shows that the model has a certain robustness to the added noise. The MAE significantly increased when σ reached 1.00. Since the peak-to-peak value of the angle is approximately 30° and the probability that the value of $\mathrm{N}\left(0, 1^2\right)$ falls within $(-3°, 3°)$ is approximately 99.74%, the maximum allowable inaccuracy of amplitude measurement is approximately 10%.

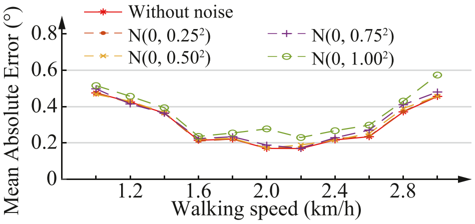

Fig. 16. Robustness test (with and without Gaussian noise).

E. Limitations

Although the experimental results are encouraging in this study, limitations still exist. First, the network only used the gaits of a single hip joint, although using the gaits of multiple lower limb joints may produce a more comprehensive study. Second, due to the variability of walking gaits, more gait datasets may be acquired for training and the complexity of the network may be increased to learn more prior experience. Third, the length of the output sequence or the sampling time of the gaits may be changed to study whether a longer-time gait can be predicted to facilitate the design of the controller. Besides, compared with nonDNN approaches, the DNN-based method not only requires the wearer to have or partially have the ability to walk for gait collection, but also increases the training expense (approximately 1 h for training 1 model). Hardware acceleration measures are needed with the enlargement of data.

VI. Conclusion

In this study, a novel neural network that combines the "sequence to sequence" structure and gated and adaptive continuous-time recurrent neural network, named S2S-GACTRNN, was proposed to process periodic signals, including sinusoidal signals with different frequencies and walking gait signals at different speeds. Simulation experiments of sinusoidal signals with different frequencies and offline experiments and online experiments of walking gait signals at different speeds were carried out to evaluate the model's learning and generalization capability respectively. The final online experimental results showed that the mean absolute errors of S2S-GACTRNN trained using walking data at three speeds were reduced by 24%, 38%, and 24% compared with that trained using walking data at one speed. The S2S-GACTRNN has the potential for walking speed learning and generalization, and the generalization performance may be improved by using more training data. The S2S-GACTRNN may be utilized as a new method for the speed-adaptation control of exoskeletons to provide users with corresponding assistance at different speeds in their daily lives.

Authorized licensed use limited to: BEIHANG UNIVERSITY. Downloaded on February 17,2023 at 11:37:53 UTC from IEEE Xplore. Restrictions apply.

This article has been accepted for inclusion in a future issue of this journal. Content is final as presented, with the exception of pagination.

Acknowledgment

The authors would like to thank Di Shi and Yixin Shao for their encouragement and support.

References

[1] D. Pinto-Fernandez et al., "Performance evaluation of lower limb exoskeletons: A systematic review," *IEEE Trans. Neural Syst. Rehabil. Eng.*, vol. 28, no. 7, pp. 1573–1583, Jul. 2020.

[2] Q. Wei, Z. Li, K. Zhao, Y. Kang, and C.-Y. Su, "Synergy-based control of assistive lower-limb exoskeletons by skill transfer," *IEEE/ASME Trans. Mechatronics*, vol. 25, no. 2, pp. 705–715, Apr. 2020.

[3] H. Yu, S. Huang, G. Chen, Y. Pan, and Z. Guo, "Human–robot interaction control of rehabilitation robots with series elastic actuators," *IEEE Trans. Robot.*, vol. 31, no. 5, pp. 1089–1100, Oct. 2015.

[4] L. Zhou, W. Chen, J. Wang, S. Bai, H. Yu, and Y. Zhang, "A novel precision measuring parallel mechanism for the closed-loop control of a biologically inspired lower limb exoskeleton," *IEEE/ASME Trans. Mechatronics*, vol. 23, no. 6, pp. 2693–2703, Dec. 2018.

[5] B. Brahmi, M. Saad, C. Ochoa-Luna, M. H. Rahman, and A. Brahmi, "Adaptive tracking control of an exoskeleton robot with uncertain dynamics based on estimated time-delay control," *IEEE/ASME Trans. Mechatronics*, vol. 23, no. 2, pp. 575–585, Apr. 2018.

[6] H. T. Tran et al., "Evaluation of a fuzzy-based impedance control strategy on a powered lower exoskeleton," *Int. J. Social Robot.*, vol. 8, no. 1, pp. 103–123, 2016.

[7] L. Teng, M. A. Gull, and S. Bai, "Pd-based fuzzy sliding mode control of a wheelchair exoskeleton robot," *IEEE/ASME Trans. Mechatronics*, vol. 25, no. 5, pp. 2546–2555, Oct. 2020.

[8] A. Duschau-Wicke et al., "Path control: A method for patient-cooperative robot-aided gait rehabilitation," *IEEE Trans. Neural Syst. Rehabil. Eng.*, vol. 18, no. 1, pp. 38–48, Feb. 2010.

[9] G. M. Gasparri, J. Luque, and Z. F. Lerner, "Proportional joint-moment control for instantaneously adaptive ankle exoskeleton assistance," *IEEE Trans. Neural Syst. Rehabil. Eng.*, vol. 27, no. 4, pp. 751–759, Apr. 2019.

[10] M. Grimmer et al., "A powered prosthetic ankle joint for walking and running," *BioMed. Eng. Online*, vol. 15, no. 3, pp. 37–52, 2016.

[11] A. Agrawal et al., "First steps towards translating hzd control of bipedal robots to decentralized control of exoskeletons," *IEEE Access*, vol. 5, pp. 9919–9934, 2017.

[12] Y. Yuan, Z. Li, T. Zhao, and D. Gan, "Dmp-based motion generation for a walking exoskeleton robot using reinforcement learning," *IEEE Trans. Ind. Electron.*, vol. 67, no. 5, pp. 3830–3839, May 2020.

[13] H. Vallery, E. H. Van Asseldonk, M. Buss, and H. Van Der Kooij, "Reference trajectory generation for rehabilitation robots: Complementary limb motion estimation," *IEEE Trans. Neural Syst. Rehabil. Eng.*, vol. 17, no. 1, pp. 23–30, Mar. 2008.

[14] R. Ronsse et al., "Oscillator-based assistance of cyclical movements: Model-based and model-free approaches," *Med. Biol. Eng. Comput.*, vol. 49, no. 10, pp. 1173–1185, 2011.

[15] E. Zheng, S. Manca, T. Yan, A. Parri, N. Vitiello, and Q. Wang, "Gait phase estimation based on noncontact capacitive sensing and adaptive oscillators," *IEEE Trans. Biomed. Eng.*, vol. 64, no. 10, pp. 2419–2430, Oct. 2017.

[16] S. Crea et al., "Controlling a robotic hip exoskeleton with noncontact capacitive sensors," *IEEE/ASME Trans. Mechatronics*, vol. 24, no. 5, pp. 2227–2235, Oct. 2019.

[17] T. Yan, A. Parri, V. R. Garate, M. Cempini, R. Ronsse, and N. Vitiello, "An oscillator-based smooth real-time estimate of gait phase for wearable robotics," *Auton. Robot.*, vol. 41, no. 3, pp. 759–774, 2017.

[18] D. Xu and Q. Wang, "Noninvasive human-prosthesis interfaces for locomotion intent recognition: A review," *Cyborg Bionic Syst.*, vol. 2021, pp. 1–14, 2021.

[19] K. Kamali, A. A. Akbari, and A. Akbarzadeh, "Trajectory generation and control of a knee exoskeleton based on dynamic movement primitives for sit-to-stand assistance," *Adv. Robot.*, vol. 30, no. 13, pp. 846–860, 2016.

[20] O. I. Abiodun, A. Jantan, A. E. Omolara, K. V. Dada, N. A. Mohamed, and H. Arshad, "State-of-the-art in artificial neural network applications: A survey," *Heliyon*, vol. 4, no. 11, 2018, Art. no. e00938.

[21] I. Kang, P. Kunapuli, and A. J. Young, "Real-time neural network-based gait phase estimation using a robotic hip exoskeleton," *IEEE Trans. Med. Robot. Bionics*, vol. 2, no. 1, pp. 28–37, Feb. 2020.

[22] X. Wu, Y. Yuan, X. Zhang, C. Wang, T. Xu, and D. Tao, "Gait phase classification for a lower limb exoskeleton system based on a graph convolutional network model," *IEEE Trans. Ind. Electron.*, vol. 69, no. 5, pp. 4999–5008, May 2022.

[23] Y. Yamanoi, S. Togo, Y. Jiang, and H. Yokoi, "Learning data correction for myoelectric hand based on "survival of the fittest"," *Cyborg Bionic Syst.*, vol. 2021, pp. 1–12, 2021.

[24] J. Namikawa, R. Nishimoto, H. Arie, and J. Tani, "Synthetic approach to understanding meta-level cognition of predictability in generating cooperative behavior," in *Advances in Cognitive Neurodynamics (III)*. Berlin, Germany: Springer, 2013, pp. 615–621.

[25] S. Murata, J. Namikawa, H. Arie, S. Sugano, and J. Tani, "Learning to reproduce fluctuating time series by inferring their time-dependent stochastic properties: Application in robot learning via tutoring," *IEEE Trans. Auto. Ment. Develop.*, vol. 5, no. 4, pp. 298–310, Dec. 2013.

[26] A. Philippsen and Y. Nagai, "A predictive coding model of representational drawing in human children and chimpanzees," in *Proc. IEEE 9 rd Joint Int. Conf. Develop. Learn. Epigenetic Robot.*, 2019, pp. 171–176.

[27] S. Heinrich, T. Alpay, and S. Wermter, "Adaptive and variational continuous time recurrent neural networks," in *Proc. Joint IEEE 8th Int. Conf. Develop. Learn. Epigenetic Robot.*, 2018, pp. 13–18.

[28] S. Heinrich, T. Alpay, and Y. Nagai, "Learning timescales in gated and adaptive continuous time recurrent neural networks," in *Proc. IEEE Int. Conf. Syst, Man Cybern.*, 2020, pp. 2662–2667.

[29] S. Hisamoto, M. Post, and K. Duh, "Membership inference attacks on sequence-to-sequence models: Is my data in your machine translation system?," *Trans. Assoc. Comput. Linguistics*, vol. 8, pp. 49–63, 2020.

[30] I. Sutskever, O. Vinyals, and Q. V. Le, "Sequence to sequence learning with neural networks," *Proc. Adv. Neural Inf. Process. Syst.*, vol. 27, 2014.

[31] A. Hirose and S. Yoshida, "Generalization characteristics of complex-valued feedforward neural networks in relation to signal coherence," *IEEE Trans. Neural Netw. Learn. Syst.*, vol. 23, no. 4, pp. 541–551, Apr. 2012.

[32] E. Trigili et al., "Design and experimental characterization of a shoulder-elbow exoskeleton with compliant joints for post-stroke rehabilitation," *IEEE/ASME Trans. Mechatronics*, vol. 24, no. 4, pp. 1485–1496, Aug. 2019.

[33] B. Hu, Z.-H. Guan, G. Chen, and C. P. Chen, "Neuroscience and network dynamics toward brain-inspired intelligence," *IEEE Trans. Cybern.*, vol. 52, no. 10, pp. 10214–10227, Oct. 2022.

[34] B. A. Wright and Y. Zhang, "A review of the generalization of auditory learning," *Philos. Trans. R. Soc. Lond. B. Biol. Sci.*, vol. 364, no. 1515, pp. 301–311, 2009.

[35] D. Hodges and M. Thaut, *The Oxford Handbook of Music and the Brain*. Oxford, U.K.: Oxford Univ. Press, 2019.

[36] A. K. Engel, C. Gerloff, C. C. Hilgetag, and G. Nolte, "Intrinsic coupling modes: Multiscale interactions in ongoing brain activity," *Neuron*, vol. 80, no. 4, pp. 867–886, 2013.

[37] L. L. Gollo et al., "Dwelling quietly in the rich club: Brain network determinants of slow cortical fluctuations," *Philos. Trans. R. Soc. Lond. B. Biol. Sci.*, vol. 370, no. 1668, 2015, Art. no. 20140165.

[38] E. Pellicano and D. Burr, "When the world becomes 'too real': A Bayesian explanation of autistic perception," *Trends Cogn. Sci.*, vol. 16, no. 10, pp. 504–510, 2012.

[39] U. E. Ogenyi, J. Liu, C. Yang, Z. Ju, and H. Liu, "Physical human–robot collaboration: Robotic systems, learning methods, collaborative strategies, sensors, and actuators," *IEEE Trans. Cybern.*, vol. 51, no. 4, pp. 1888–1901, Apr. 2021.

[40] T. Yang and X. Gao, "Adaptive neural sliding-mode controller for alternative control strategies in lower limb rehabilitation," *IEEE Trans. Neural Syst. Rehabil. Eng.*, vol. 28, no. 1, pp. 238–247, Jan. 2020.

Wuxiang Zhang (Member, IEEE) received the M.Sc. degree in mechatronics engineering from the Huazhong University of Science and Technology, Wuhan, China, in 2004 and the Ph.D. degree in mechatronics engineering from the Beihang University, Beijing, China, in 2009.

He is currently a Professor of mechanisms and machine science with the School of Mechanical Engineering and Automation, Beihang University. His research interests include variable topology mechanisms, exoskeleton robot, space robot, and industrial automation.

Authorized licensed use limited to: BEIHANG UNIVERSITY. Downloaded on February 17,2023 at 11:37:53 UTC from IEEE Xplore. Restrictions apply.

This article has been accepted for inclusion in a future issue of this journal. Content is final as presented, with the exception of pagination.

Zhitao Ling received the B.S. degree in mechanical engineering in 2020 from Beihang University, Beijing, China, where he is currently working toward the M.S. degree in mechanical engineering with the School of Mechanical Engineering and Automation.

Stefan Heinrich received the Ph.D. degree in computer science from the Department of Informatics, University of Hamburg, Hamburg, Germany, in 2016.

He is currently an Assistant Professor with the Department of Computer Science, IT University of Copenhagen, Copenhagen, Denmark, where he studies temporal dynamic information-processing mechanisms between cognitive modeling and machine learning.

Xilun Ding received the B.Eng. degree in mechanical engineering from the Zhengzhou Institute of Technology, Zhengzhou, China, in 1991, and the M.Eng. degree in mechanical design and the Ph.D. degree in mechatronics and automation from the Harbin Institute of Technology, Harbin, China, in 1994 and 1997, respectively.

His research interests include the dynamics of compliant mechanical systems and robots, nonholonomic control of space robots, dynamics and control of aerial robots, and biomimetic robots.

Yanggang Feng (Member, IEEE) received the Ph.D. degree in dynamics and control from the College of Engineering, Peking University, Beijing, China, in 2019.

Subsequently, he joined the University of Tokyo, Tokyo, Japan, as a Postdoctoral Researcher. He is currently an Assistant Professor with the School of Mechanical Engineering and Automation, Beihang University, Beijing, China. His research interests include wearable robotics and AI.

Authorized licensed use limited to: BEIHANG UNIVERSITY. Downloaded on February 17,2023 at 11:37:53 UTC from IEEE Xplore. Restrictions apply.